# Supporting Information

## Purohit et al. 10.1073/pnas.1203633109

### SI Methods

**Cell Culture and Mutagenesis.** HEK 293 cells were maintained in DMEM supplemented with 10% (vol/vol) FBS and 1% (vol/vol) penicillin-streptomycin (pH 7.4). The cultures were incubated at 37 °C and 5% (vol/vol) $CO_2$. The QuikChange site-directed mutagenesis kit (Stratagene) was used to create mutations that were verified by nucleotide sequencing. HEK cells were transiently transfected using the calcium phosphate precipitation method by incubating them for ∼15 h with 3.5–5.5 μg of DNA per 35-mm culture dish at the ratio of 2:1:1:1 (α/β/δ/ε). The cells were cotransfected with GFP (0.1 μg/μL) as a marker protein. Cells were washed by changing the media after ∼15 h of transfection, and electrophysiological recordings were made within ∼36 h after washing.

**Electrophysiology.** Single-channel currents were recorded in the cell-attached patch configuration at 23 °C. The composition of the bath solution was 142 mM KCl, 5.4 mM NaCl, 1.8 mM $CaCl_2$, 1.7 mM $MgCl_2$, and 10 mM Hepes/KOH (pH 7.4). The patch pipettes were filled with Dulbecco's PBS containing 137 mM NaCl, 0.9 mM $CaCl_2$, 2.7 mM KCl, 1.5 mM $KH_2PO_4$, 0.5 mM $MgCl_2$, and 8.1 mM $Na_2HPO_4$ (pH 7.3, NaOH). For the experiments with agonists, ACh was added only to the pipette solution. Stock ACh solution was diluted using either regular or modified (NaCl-free) Dulbecco's PBS. Patch pipettes (∼10 MΩ) were fabricated from borosilicate glass and coated with Sylgard (Dow Corning). Single-channel currents were acquired using a Warner PC505B amplifier (Warner Instruments), low-pass-filtered at 20 kHz using an LPF-8 external filter (Warner Instruments), and digitized at a sampling frequency of 50 kHz using an SCB-68 data acquisition board (National Instruments). The wire and pipette holder used in unliganded studies was never exposed to agonists.

**Kinetic Modeling.** Kinetic analysis of single-channel data was performed using QUB software (www.qub.buffalo.edu). At sufficiently high agonist concentrations, channel openings occurred in clusters, where each cluster represented the binding and gating activity of a single AChR and the silent intervals between clusters represented epochs when all the AChRs in the patch were desensitized. For estimation of the rate constants, clusters of openings flanked by ≥∼20-ms silent periods were selected by eye. Currents within clusters were idealized into noise-free intervals after further digital low-pass filtering at 12 kHz (unliganded currents were not filtered), using the segmental *k*-means algorithm (1). The diliganded or unliganded forward ($f_2$ or $f_0$) and backward ($b_2$ or $b_0$) gating rate constants were estimated from the idealized interval durations by using the maximum-interval likelihood algorithm after imposing a dead time of 25 μs (2). The diliganded or unliganded gating equilibrium constant ($E_2$ or $E_0$) is the ratio of corresponding f/b rate constants.

In diliganded experiments, the interval durations obtained at saturating [ACh] (below) were fitted by a reaction scheme that had a gating step (C ↔ O) plus a step to account for occasional sojourns in short-lived desensitized states, with the added nonconducting state attached to O. In unliganded experiments, the idealized intracluster interval durations were first fitted using a two-state model (C ↔ O). For almost all the binding site mutants, the unliganded open and closed intervals could be described by means of this simple scheme. When this was not the case, additional C and O states were added to the model, one at a time, until the log-likelihood score failed to improve by >10 units. The rates, $f_0$ and $b_0$, were computed as the inverse of the predominant closed- and open-lifetime components.

**$E_2$ Estimation.** At low agonist concentrations (<∼3 $K_d$), the durations of intervals within clusters of single-channel currents are influenced by both agonist binding and channel gating. To obtain the $E_2$ estimates, higher [ACh] values were used to eliminate the binding events (which were almost all shorter than the dead time). ACh is a channel blocker, and at [ACh] >∼0.5 mM, current flow through the channel is significantly reduced. To reduce channel block, we depolarized the membrane to +100 mV, and to compensate for the effect of depolarization on gating (which is the same for $E_2$ and $E_0$), we added the mutation εS450W (in M4 of the ε-subunit), which has no effect on $K_d$ or $\Delta G_B$ (3). Under these conditions, the currents were in the outward direction but the rate and equilibrium constants pertain to AChRs at −100 mV.

To be sure that the rate constants reflected only gating, it was essential to ascertain whether or not binding site saturation by the agonist had been achieved. We made this determination by comparing the apparent opening rate (the inverse of the predominant intracluster closed interval duration component) at different [ACh] values. If this rate did not increase with a further increase in [ACh], we concluded that saturation had been achieved. For some mutants, the plateau in the apparent opening rate was reached at 10–30 mM, but we typically compared this value at 100 mM vs. 140 mM ACh to assess saturation. The $f_2$ estimate was the effective opening rate at saturation, and the $b_2$ estimate was the effective closing rate at 10 mM ACh (where no channel block was apparent). The rate constants are shown in Table S2.

A further problem with $E_2$ estimation is that some mutations reduce $f_2$ to an extent to which clusters could not be clearly defined. For these, we added additional background mutations that increased $f_2$ but had no effect on $K_d^{ACh}$ or $\Delta G_B^{ACh}$, namely, εS450A, εL269F, ε(L269F + E181W), and αD97A + αY127F (Table S7). The observed rate constants were corrected according to the background used. Both the observed and background-corrected values are given in the tables.

**$E_0$ Estimation.** The method we used to estimate $E_0$ is described in detail elsewhere (4). Briefly, background mutations were used to increase the frequency of unliganded openings so that they occurred in clusters and $E_0^{bkg}$ could be measured for individual AChRs. The background combination was αD97A + αS269I + αY127F (DYS). Each of these mutations increases $E_0$ without affecting $K_d$ or $\Delta G_B$. The aromatic mutations were expressed, one at a time, on the DYS background, and the unliganded gating equilibrium constant was measured experimentally ($E_0^{mut+bkg}$). We then calculated the fold-change in $E_0$ caused by the aromatic mutation as $E_0^{mut+bkg}/E_0^{bkg}$. We estimate that $E_0^{wt} = 7.0 \times 10^{-7}$; thus, $E_0$ for just the aromatic mutant ($E_0^{mut}$) was computed by multiplying the fold change by $7 \times 10^{-7}$. Newly measured (previously unpublished) $E_0^{mut}$ values are provided in Table S5.

**$\Delta G_B$ Estimation.** From measurements of $E_2^{ACh}$ and $E_0^{mut}$, we define (Fig. S1) $2\Delta G_B^{ACh}$ (kcal/mol) = $-0.59 \ln(K_d/J_d)$. $2\Delta G_B^{ACh}$ gives the total energy from both sites combined, and the $\Delta G_B^{ACh}$ values we report are the average of the single-site energies.

We estimated the error limits in $\Delta G_B^{ACh}$, which is the natural log of a square root of a ratio, as follows. $(K_d/J_d)^2$ (=λ) was calculated from the division of two experimental variables,

$E_2/E_0$. The error in this ratio is $s_\lambda^2 = \lambda^2 \cdot \sqrt{[(s_{E2}/E_2)^2 + (s_{E0}/E_0)^2]}$, where $s_x$ is the associated SEM of each equilibrium constant (Table S1). λ was calculated as the square root of $E_2/E_0$, which has an associated error of $s_\lambda = (0.5 \cdot \lambda) \cdot (s_\lambda^2/\lambda^2)$. $\Delta G_B$ is proportional to the natural logarithm λ, which has an associated error of $s_\Lambda = s_\lambda/\lambda$. For example, for TrpB-Y, $E_2 = 1.43 \pm 0.23$ and $E_0 = 2.1 \pm 0.3 \times 10^{-6}$. Using the above method, we calculate $\lambda^2 = 6.9 \pm 1.5 \times 10^5$, $\lambda = 828 \pm 89$, and $\Delta G_B^{ACh} = -4.0 \pm 0.06$ kcal/mol.

We also estimated interaction energies for some double-mutant constructs. The coupling free energy was calculated as $\Delta G_B^{dbl}/(\Delta G_B^{mut1} - \Delta G_B^{mut2})$.


1. Qin F (2004) Restoration of single-channel currents using the segmental k-means method based on hidden Markov modeling. *Biophys J* 86:1488–1501.
2. Qin F, Auerbach A, Sachs F (1997) Maximum likelihood estimation of aggregated Markov processes. *Proc Biol Sci* 264:375–383.
3. Jadey SV, Purohit P, Bruhova I, Gregg TM, Auerbach A (2011) Design and control of acetylcholine receptor conformational change. *Proc Natl Acad Sci USA* 108:4328–4333.
4. Purohit P, Auerbach A (2009) Unliganded gating of acetylcholine receptor channels. *Proc Natl Acad Sci USA* 106:115–120.


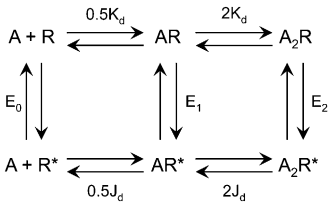


**Fig. S1.** Cyclical activation scheme for the AChR. A is the agonist, and the other letters represent stable ground states. Paired arrows represent the unstable intermediates that connect the ground states. R indicates resting conformation (low affinity for the agonist and low ionic conductance), and R* indicates active conformation (high affinity for the agonist and high ionic conductance). Next to the arrows are the salient equilibrium constants. $E_0$, unliganded (constitutive) gating; $E_1$, monoliganded gating; $E_2$, diliganded gating; $K_d$, dissociation constant for agonist binding to R; $J_d$, dissociation constant for agonist binding to R*. The two wt binding sites have approximately the same $K_d$ and $J_d$ for ACh (1). Without an external energy source, the net energy change, R to $A_2R^*$, must be equal for the common "physiological" pathway ($R \leftrightarrow AR \leftrightarrow A_2R \leftrightarrow A_2R^*$) and for the rarely taken alternative pathway ($R \leftrightarrow R^* \leftrightarrow AR^* \leftrightarrow A_2R^*$). Hence, $E_2/K_d^2 = E_0/J_d^2$.


1. Jha A, Auerbach A (2010) Acetylcholine receptor channels activated by a single agonist molecule. *Biophys J* 98:1840–1846.

**Table S1. Energy estimates for aromatic mutants**

| Construct | $E_2$ (±) SEM | $E_0$* (±) SEM | $(\sqrt{(E_2/E_0)})^{ACh}$ (±) SEM | $\Delta G_B^{ACh}$ (±) SEM, kcal/mol | $\Delta\Delta G_B^{ACh}$, kcal/mol |
|---|---|---|---|---|---|
| wt | 25.4 | 7.0E-07 | 6,024 | −5.14 | |
| TrpB-Y | 1.43 ± 0.23 | 2.1E-06 ± 3.E-07 | 828 ± 89 | −3.96 ± −0.06 | 1.18 |
| F | 1.13 ± 0.1 | 2.3E-06 ± 3.E-07 | 689 ± 53 | −3.86 ± −0.05 | 1.28 |
| H | 0.01 ± 4.0E-05 | 1.0E-07 ± 1.E-08 | 310 ± 22 | −3.38 ± −0.04 | 1.76 |
| T† | 0.18 ± 0.04 | 8.0E-06 ± | 150 ± | −2.96 ± | 2.18 |
| V† | 0.06 ± 8.0E-03 | 3.6E-06 ± | 130 ± | −2.87 ± | 2.27 |
| C† | 0.52 ± 0.07 | 3.8E-05 ± | 118 ± | −2.81 ± | 2.33 |
| A | 0.07 ± 3.0E-03 | 5.5E-06 ± 3.E-08 | 111 ± 2 | −2.78 ± −0.01 | 2.36 |
| S | 0.10 ± 4.0E-04 | 1.0E-05 ± 1.E-07 | 98 ± 1 | −2.70 ± 0.00 | 2.44 |
| M† | 2.5E-03 ± 3.0E-04 | 4.6E-07 ± 1.E-08 | 74 ± 5 | −2.54 ± −0.04 | 2.60 |
| N† | 9.0E-03 ± 2.0E-03 | 2.1E-06 ± 1.E-07 | 66 ± 8 | −2.47 ± −0.07 | 2.67 |
| TyrC1-F | 0.02 ± 0.002 | 4.1E-07 ± 7.E-08 | 216 ± 22 | −3.17 ± −0.06 | 1.97 |
| W | 0.01 ± 0.0003 | 9.5E-07 ± 2.E-07 | 122 ± 12 | −2.83 ± −0.06 | 2.31 |
| H | 3.0E-04 ± 4.0E-05 | 5.5E-07 ± 6.E-08 | 23 ± 2 | −1.86 ± −0.05 | 3.28 |
| S | 1.2E-04 ± 8.0E-06 | 3.1E-07 ± 6.E-08 | 20 ± 2 | −1.76 ± −0.06 | 3.38 |
| A | 5.3E-05 ± 3.1E-06 | 6.3E-07 ± 6.E-08 | 9 ± 1 | −1.31 ± −0.03 | 3.83 |
| TyrC2-F | 14.02 ± 6.20 | 6.1E-07 ± 9.E-08 | 4,784 ± 1112 | −5.00 ± −0.14 | 0.14 |
| W | 0.89 ± 0.29 | 1.8E-06 ± 7.E-08 | 712 ± 117 | −3.87 ± −0.10 | 1.27 |
| H | 0.26 ± 0.13 | 6.7E-07 ± 9.E-08 | 621 ± 161 | −3.79 ± −0.15 | 1.35 |
| N | 0.07 ± 0.04 | 3.5E-07 ± 4.E-08 | 439 ± 131 | −3.59 ± −0.17 | 1.55 |
| S | 0.11 ± 0.03 | 9.9E-07 ± 3.E-07 | 330 ± 63 | −3.42 ± −0.11 | 1.72 |
| T | 0.05 ± 0.01 | 8.2E-07 ± 1.E-09 | 251 ± 25 | −3.26 ± −0.06 | 1.88 |
| A | 0.03 ± 0.01 | 8.3E-07 ± 1.E-07 | 179 ± 35 | −3.06 ± −0.11 | 2.08 |
| L | 1.4E-03 ± 3.7E-04 | 7.7E-07 ± 4.E-08 | 43 ± 6 | −2.22 ± −0.08 | 2.92 |
| TyrA-F | 0.67 ± 0.02 | 8.2E-08 ± 1.E-08 | 2,864 ± 259 | −4.70 ± −0.05 | 0.44 |
| W | 0.54 ± 0.06 | 1.8E-07 ± 1.E-08 | 1,757 ± 122 | −4.41 ± −0.04 | 0.73 |
| E | 0.18 ± 0.01 | 1.0E-07 ± 1.E-08 | 1,328 ± 102 | −4.24 ± −0.05 | 0.90 |
| H | 1.83 ± 0.15 | 1.5E-06 ± 1.E-07 | 1,120 ± 64 | −4.14 ± −0.03 | 1.00 |
| C | 0.06 ± 0.01 | 5.8E-08 ± 1.E-08 | 1,014 ± 132 | −4.08 ± −0.08 | 1.06 |
| A | 0.58 ± 0.02 | 6.6E-07 ± 3.E-08 | 940 ± 26 | −4.04 ± −0.02 | 1.10 |
| G | 0.13 ± 0.03 | 4.7E-07 ± 1.E-08 | 528 ± 61 | −3.70 ± −0.07 | 1.44 |
| S | 0.16 ± 0.01 | 8.3E-07 ± 4.E-08 | 439 ± 18 | −3.59 ± −0.02 | 1.55 |
| T | 0.01 ± 0.001 | 9.5E-08 ± 1.E-08 | 325 ± 30 | −3.41 ± −0.05 | 1.73 |

TrpB, TyrC1, TyrC2, and TyrA correspond to W149, Y190, Y198, and Y93 in the AChR mouse α-subunit. $\Delta G_B^{ACh} = -0.59 \cdot \ln[\sqrt{(E_2/E_0)}]$, $\Delta\Delta G_B = \Delta G_B^{ACh,\,mut} - \Delta G_B^{ACh,\,wt}$.

*Previously published $E_0$ measurements (1) corrected here for an $E_0^{wt}$ value of $7 \times 10^{-7}$.

†Previously published $E_2$ measurements (2).


1. Purohit P, Auerbach A (2010) Energetics of gating at the apo-acetylcholine receptor transmitter binding site. *J Gen Physiol* 135:321–331.
2. Purohit P, Auerbach A (2011) Glycine hinges with opposing actions at the acetylcholine receptor-channel transmitter binding site. *Mol Pharmacol* 79:351–359.

**Table S2. Observed and corrected rate/equilibrium constants**

| | Measured | | | Background-corrected | | | |
|---|---|---|---|---|---|---|---|
| Construct | $f_2$ | $b_2$ | $E_2$ | $f_2$ | $b_2$ | $E_2$ | *n* |
| wt (ACh)* | | | | 65,850 | 2,595 | 25.40 | — |
| TrpB-Y[†] | 1,938 ± 307 | 1,670 ± 648 | 1.16 ± 0.18 | 2,236 ± 354 | 1,569 ± 609 | 1.43 ± 0.23 | 3 |
| F[†] | 1,939 ± 170 | 2,111 ± 326 | 0.92 ± 0.01 | 2,237 ± 196 | 1,984 ± 307 | 1.13 ± 0.1 | 8 |
| C[‡] | | | | 287 ± 42 | 554 ± 11 | 0.52 ± 0.07 | — |
| T[‡] | | | | 190 ± 18 | 1,052 ± 238 | 0.18 ± 0.04 | — |
| S[†] | 179 ± 25 | 2,266 ± 145 | 0.08 ± 0.01 | 207 ± 29 | 2,129 ± 136 | 0.10 ± 4.0E-04 | 3 |
| A[†] | 136 ± 9 | 2,282 ± 490 | 0.06 ± 0.004 | 157 ± 10 | 2,144 ± 460 | 0.07 ± 0.003 | 3 |
| V[‡] | | | | 79 ± 3 | 1,215 ± 114 | 0.06 ± 0.008 | — |
| H[§] | 147 ± 30 | 1,599 ± 35 | 0.09 ± 0.02 | 20 ± 2 | 2,678 ± 58 | 0.01 ± 4.0E-05 | 6 |
| N[‡] | | | | 15 ± 3 | 1,698 ± 129 | 0.01 ± 0.002 | — |
| M[‡] | | | | 6.3 ± 0.5 | 2,549 ± 508 | 2.5E-03 ± 3.0E-04 | — |
| TyrC1-F[§] | 1,090 ± 54 | 3,503 ± 116 | 0.31 ± 0.04 | 126 ± 6 | 5,866 ± 194 | 0.02 ± 0.002 | 4 |
| W[§] | 821 ± 87 | 4,565 ± 256 | 0.18 ± 0.02 | 108 ± 18 | 7,644 ± 424 | 0.01 ± 0.0003 | 3 |
| H[†,¶] | 5,098 ± 681 | 3,573 ± 284 | 1.43 ± 0.2 | 1.79 ± 0.2 | 5,984 ± 476 | 3.0E-04 ± 4.0E-05 | 7 |
| S[†,¶] | 1,245 ± 82 | 2,161 ± 161 | 0.58 ± 0.07 | 0.4 ± 0.03 | 3,618 ± 269 | 1.2E-04 ± 8.0E-06 | 3 |
| A[†,¶] | 1,478 ± 85 | 5,909 ± 571 | 0.25 ± 0.02 | 0.5 ± 0.03 | 9,895 ± 956 | 5.3E-05 ± 3.1E-06 | 4 |
| TyrC2-F[‖] | 2,626 ± 170 | 3,010 ± 674 | 0.87 ± 0.40 | 53,249 ± 3,449 | 3,799 ± 851 | 14.02 ± 6.20 | 10 |
| W[**] | 1,685 ± 315 | 1,407 ± 185 | 1.20 ± 0.39 | 1,352 ± 253 | 1,525 ± 201 | 0.89 ± 0.29 | 4 |
| H[**] | 727 ± 164 | 2,078 ± 49 | 0.35 ± 0.18 | 583 ± 164 | 2,253 ± 53 | 0.26 ± 0.13 | 2 |
| S[**] | 498 ± 32 | 3,412 ± 52 | 0.15 ± 0.06 | 399 ± 26 | 3,700 ± 57 | 0.11 ± 0.04 | 4 |
| N[**] | 229 ± 15 | 2,519 ± 370 | 0.09 ± 0.03 | 184 ± 12 | 2,731 ± 401 | 0.07 ± 0.03 | 3 |
| T[§] | 1,225 ± 152 | 1,675 ± 524 | 0.73 ± 0.12 | 141 ± 18 | 2,744 ± 858 | 0.05 ± 0.01 | 3 |
| A[§] | 710 ± 38 | 1,882 ± 521 | 0.38 ± 0.13 | 82 ± 4 | 3,084 ± 854 | 0.03 ± 0.01 | 4 |
| L[††] | 545 ± 94 | 3,151 ± 606 | 0.17 ± 0.04 | 2.4 ± 0.4 | 1,670 ± 321 | 1.4E-03 ± 3.7E-04 | 5 |
| TyrA-H[†] | 4,235 ± 218 | 2,729 ± 178 | 1.55 ± 0.08 | 4,703 ± 380 | 2,565 ± 433 | 1.83 ± 0.15 | 3 |
| F[†] | 115 ± 39 | 2,108 ± 168 | 0.05 ± 0.02 | 1,333 ± 45 | 1,981 ± 158 | 0.67 ± 0.02 | 3 |
| A[†] | 1,009 ± 34 | 2,134 ± 55 | 0.47 ± 0.02 | 1,164 ± 40 | 2,006 ± 52 | 0.58 ± 0.02 | 3 |
| W[†] | 1,003 ± 123 | 2,292 ± 674 | 0.44 ± 0.09 | 1,158 ± 142 | 2,154 ± 634 | 0.54 ± 0.06 | 3 |
| E[†] | 381 ± 32 | 2,592 ± 55 | 0.15 ± 0.01 | 439 ± 37 | 2,436 ± 52 | 0.18 ± 0.01 | 3 |
| S[†] | 570 ± 24 | 4,395 ± 889 | 0.13 ± 0.005 | 658 ± 27 | 4,130 ± 835 | 0.16 ± 0.01 | 3 |
| G[†] | 430 ± 108 | 4,213 ± 3 | 0.10 ± 0.03 | 497 ± 124 | 3,959 ± 400 | 0.13 ± 0.03 | 3 |
| C[†] | 145 ± 31 | 3,081 ± 154 | 0.05 ± 0.01 | 167 ± 36 | 2,895 ± 145 | 0.06 ± 0.01 | 3 |
| T[§] | 559 ± 80 | 3,899 ± 326 | 0.14 ± 0.02 | 65 ± 9 | 6,530 ± 546 | 0.01 ± 0.001 | 3 |

TrpB, TyrC1, TyrC2, and TyrA correspond to W149, Y190, Y198, and Y93 in the AChR mouse α subunit. *n*, number of patches.
*Measurements from Jadey et al. (1).
[†]Background mutant εS450W.
[‡]Data from Purohit and Auerbach (2).
[§]Background mutant εL269F.
[¶]Background mutant α(D97A + Y127F).
[‖]Background mutant εS450W + δI43H.
**Background mutant εS450A.
[††]Background mutant ε(L269F + E181W).

1. Jadey SV, Purohit P, Bruhova I, Gregg TM, Auerbach A (2011) Design and control of acetylcholine receptor conformational change. *Proc Natl Acad Sci USA* 108:4328–4333.
2. Purohit P, Auerbach A (2011) Glycine hinges with opposing actions at the acetylcholine receptor-channel transmitter binding site. *Mol Pharmacol* 79:351–359.

**Table S3. Φ-Values of aromatic residues**

| | Φ-Values | |
|---|---|---|
| Position | Diliganded | Unliganded |
| TrpB | 0.97 ± 0.05 | 0.81 ± 0.04 |
| TyrC1 | 0.94 ± 0.03 | 0.89 ± 0.10 |
| TyrC2 | 1.00 ± 0.03 | 0.70 ± 0.06 |
| TyrA | 0.89 ± 0.04 | 0.83 ± 0.04 |

**Table S4. Interaction energies of F/F and S/S mutant pairs for aromatic residues**

| Construct | $E_2^{ACh}$ (±) SEM | $E_0^{obs}$ (±) SEM | $E_0^{calc}$ (±) SEM | $(\sqrt{(E_2/E_0)})^{ACh}$ (±) SEM | $\Delta G_B^{ACh}$ (±) SEM | | |
|---|---|---|---|---|---|---|---|
| | | | | | Measured | Expected | Interaction energy |
| αTyrA-F + αTrpB-F | 0.015 ± 1.1E-03 | 0.014 ± 0.0030 | 2.1E-07 ± 1.6E-08 | 270 ± 14.2 | −3.30 ± 0.03 | −3.42 | 0.12 |
| αTyrA-F + αTyrC1-F | 7.1E-04 ± 5.4E-05 | 0.007 ± 1.9E-05 | 9.6E-08 ± 2.8E-10 | 86 ± 3.3 | −2.63 ± 0.02 | −2.73 | 0.10 |
| αTyrA-F + αTyrC2-F | 0.169 ± 3.5E-02 | 0.007 ± 0.0026 | 1.1E-07 ± 1.4E-08 | 1,267 ± 154.3 | −4.22 ± 0.07 | −4.56 | 0.34 |
| αTrpB-F + αTyrC1-F | 0.001 ± 1.1E-04 | 0.047 ± 0.0074 | 6.9E-07 ± 1.1E-07 | 39 ± 3.7 | −2.16 ± 0.05 | −1.89 | −0.27 |
| αTrpB-F + αTyrC2-F | 0.190 ± 2.9E-02 | 0.088 ± 0.0185 | 1.3E-06 ± 1.3E-07 | 385 ± 35.4 | −3.51 ± 0.05 | −3.72 | 0.21 |
| αTyrC1-F + αTyrC2-F | 0.028 ± 2.4E-03 | 0.014 ± 0.0043 | 2.0E-07 ± 6.3E-08 | 374 ± 60.6 | −3.49 ± 0.09 | −3.03 | −0.47 |
| αTyrA-S + αTyrC2-S | 8.3E-04 ± 1.1E-04 | 0.026* ± NA | 3.8E-07 ± NA | 47 ± NA | −2.27 ± NA | −1.87 | −0.40 |
| αTrpB-S + αTyrC2-S | 0.0015 ± 5.1E-05 | 0.930* ± 0.0250 | 1.4E-05 ± 3.6E-07 | 11 ± 0.2 | −1.41 ± 0.01 | −0.99 | −0.42 |

TrpB, TyrC1, TyrC2, and TyrA correspond to W149, Y190, Y198, and Y93 in the AChR mouse α-subunit. $E_0^{obs}$ is the unliganded gating equilibrium constant observed on the DYS background. $E_0^{calc}$ is the unliganded gating equilibrium constant corrected for the background.
*Previously published $E_0$ measurements (1).

1. Purohit P, Auerbach A (2010) Energetics of gating at the apo-acetylcholine receptor transmitter binding site. *J Gen Physiol* 135:321–331.

**Table S5. Previously unpublished $E_0$ measurements**

| Construct | $f_0$ | $b_0$ | $E_0$ | | Interaction energy, kcal/mol |
|---|---|---|---|---|---|
| | | | Observed | Expected | |
| αTyrA-F + αTrpB-F | 80 ± 5 | 5,604 ± 931 | 0.014 ± 0.0030 | 0.019 | +0.2 |
| αTyrA-F + αTyrC1-F | 158 ± 10 | 24,060 ± 1,430 | 0.007 ± 1.9E-05 | 0.003 | −0.4 |
| αTyrA-F + αTyrC2-F | 140 ± 15 | 19,387 ± 3,244 | 0.007 ± 0.0026 | 0.005 | −0.2 |
| αTrpB-F + αTyrC1-F | 275 ± 3 | 5,825 ± 838 | 0.047 ± 0.0074 | 0.092 | +0.4 |
| αTrpB-F + αTyrC2-F | 315 ± 129 | 3,577 ± 729 | 0.088 ± 0.0185 | 0.139 | +0.3 |
| αTyrC1-F + αTyrC2-F | 126 ± 24 | 9,175 ± 1,093 | 0.014 ± 0.0043 | 0.024 | +0.3 |
| αTyrC1-H | 207 ± 14 | 5,563 ± 321 | 0.038 ± 0.004 | — | |

Expected values are the products of the fold changes in $E_0$ apparent for each mutation alone (no energy coupling).

**Table S6. Energy change ($\Delta\Delta G_B^{ACh}$, kcal/mol) estimates for some mutants**

| Position | F/W → A | F/W → S | Y → F | F → W |
|---|---|---|---|---|
| TrpB | +2.4 | +2.4 | +0.1 | −1.3 |
| TyrC1 | +1.9 | +1.4 | +2.0 | +0.3 |
| TyrC2 | +1.9 | +1.5 | +0.2 | +1.1 |
| TyrA | +0.7 | +1.1 | +0.4 | +0.3 |

**Table S7. Locations and previously-published effects of mutations on $E_2$**

| Construct | Location | $E_2$ | $E_2^{mt}/E_2^{wt}$ | Ref(s). |
|---|---|---|---|---|
| αD97A | Loop A | 8.0 | 168 | (1) |
| αY127F | ECD | 2.7 | 59 | (2) |
| δI43H | ECD | 2.0 | 0.07 | (2) |
| εE181W | Loop 9 | 0.3 | 5.8 | (3) |
| εL269F | M2 | 8.3 | 179 | (4) |
| εS450A | M4 | 1.9 | 17 | (5) |
| εS450W | M4 | 1.1 | 9.9 | (5) |

ECD, extracellular domain; M2, transmembrane segment 2; M4, transmembrane segment 4.

1. Chakrapani S, Bailey TD, Auerbach A (2003) The role of loop 5 in acetylcholine receptor channel gating. *J Gen Physiol* 122:521–539.
2. Purohit P, Auerbach A (2007) Acetylcholine receptor gating: Movement in the alpha-subunit extracellular domain. *J Gen Physiol* 130:569–579.
3. Jha A, Gupta S, Zucker SN, Auerbach A (2012) The energetic consequences of loop 9 gating motions in acetylcholine receptor-channels. *J Physiol* 590(1):119–129.
4. Jha A, Purohit P, Auerbach A (2009) Energy and structure of the M2 helix in acetylcholine receptor-channel gating. *Biophys J* 96:4075–4084.
5. Mitra A, Bailey TD, Auerbach AL (2004) Structural dynamics of the M4 transmembrane segment during acetylcholine receptor gating. *Structure* 12:1909–1918.